

A Protecting Group Approach toward Au-Silica Janus Nanostars

Denis Rodríguez-Fernández, Thomas Altantzis, Hamed Heidari, Sara Bals, Luis M. Liz-Marzán*

corresponding author: lizmarzan@cicbiomagune.es

This document is the Accepted Manuscript version of a Published Work that appeared in final form in Chem Comm, copyright © RSC after peer review and technical editing by the publisher. To access the final edited and published work see:
Chem Comm, **2014**, 50, 79-81. DOI: [10.1039/C3CC47531J](https://doi.org/10.1039/C3CC47531J)

A Protecting Group Approach toward Au-Silica Janus Nanostars

Denis Rodríguez-Fernández^{a,c}, Thomas Altantzis^b, Hamed Heidari^b, Sara Bals^b, Luis M. Liz-Marzán^{a,c,d,*}

Received (in XXX, XXX) Xth XXXXXXXXX 200X, Accepted Xth XXXXXXXXX 200X

First published on the web Xth XXXXXXXXX 200X

DOI: 10.1039/b000000x

The concept of protecting groups, widely used in organic chemistry, has been applied for the synthesis of Au-Silica Janus stars, in which gold branches protrude from one half of Au-Silica Janus spheres. This configuration opens up new possibilities to apply the plasmonic properties of gold nanostars, as well as a variety of chemical functionalizations on the silica component.

Protecting groups are commonly used in organic chemistry to perform chemical reactions in the presence of other functional groups that can be affected by the process. The quest of new protecting groups with multiple properties has led synthetic protocols to a new level that allows the preparation of highly complex molecules.¹ Although protection and deprotection have been widely employed with great success at the molecular level and even with colloids larger than 100 nm, this strategy has been far less explored with small nanoparticles.^{2,3,4,5} Various molecular analogies have been proposed for the design of novel nanoscale materials, and in particular for plasmonic nanomaterials.⁶ However, whereas in organic chemistry these processes are mainly carried out in homogeneous solutions and the final products are obtained by routine techniques such as

crystallization or chromatography and solvent evaporation, when working with colloids different parameters must be considered e.g. to avoid aggregation during synthesis and recovery of the product, including the type of solvent, the nature of the nanoparticles or the stabilizing molecules, among others.

We present here a protecting group-like strategy to synthesize Janus nanoparticles, exhibiting different materials on roughly each half of the particle. Our objective was to achieve plasmonic nanoparticles that could hold different functionalities at opposite sides, while maintaining a strong optical (plasmonic) activity, for example gold nanostars⁷ in which the spikes protrude from only one half of the central sphere. Such a configuration may offer important advantages toward subsequent directed self-assembly processes or selective biofunctionalization. We thus devised a multistep procedure involving several pathways that have been previously used to synthesize patchy particles: self-assembly of ligands over a metallic surface, masking or protection and seeded growth.⁸ We first prepared 40 nm gold nanoparticles, onto which two different ligands were self-assembled to guide the growth of a silica semishell, leading to the formation of Au-SiO₂ Janus particles. Besides providing colloidal stability due to a high negative charge, the silica semishell can act as a mask to direct the subsequent seeded growth of gold spikes, exclusively on the part of the metal that remained exposed to the solution. This ultimately leads to a particle comprising a silica sphere with Au branches protruding from one side and therefore with highly anisotropic optical properties. Finally, the silica shell can also be removed if required, thus completely mimicking the behavior of protecting groups in organic chemistry. This approach is summarized in *Figure 1* and full details are provided in the *Electronic Supporting Information (ESI)*.

Also shown in *Figure 1* are representative TEM images corresponding to the different synthesis steps (Vis-NIR spectra are shown in *Figures S2 and S3, ESI*). First, ca. 40 nm citrate-capped Au spheres ($\lambda_{\text{max}} \sim 528\text{nm}$) were prepared,⁹ which could be easily transferred into alcoholic solution for growth of the silica semishells, probably due to the high concentration of citrate molecules compared to earlier methods.¹⁰ Prior to formation of the oxide layer, in a 2-propanol:water mixture (2:1) a ligand couple – 4-mercaptobenzoic acid (4-MBA) / poly-(acrylic acid) (PAA, Mw=25000g/mol) – was allowed to self-assemble over the metallic surface, resulting in significant segregation as previously reported.¹¹ Silica was then formed by means of the well-known Stöber method only on top of the 4-MBA-capped area, while PAA acted as a stabilizer over the exposed gold surface (*step 1, Figure 1; Figure S5*). These particles were stable in the synthesis solution, but could also be washed with 2-propanol to remove the excess of reactants with no apparent aggregation or particle degradation. Typical TEM images and Vis-NIR spectra

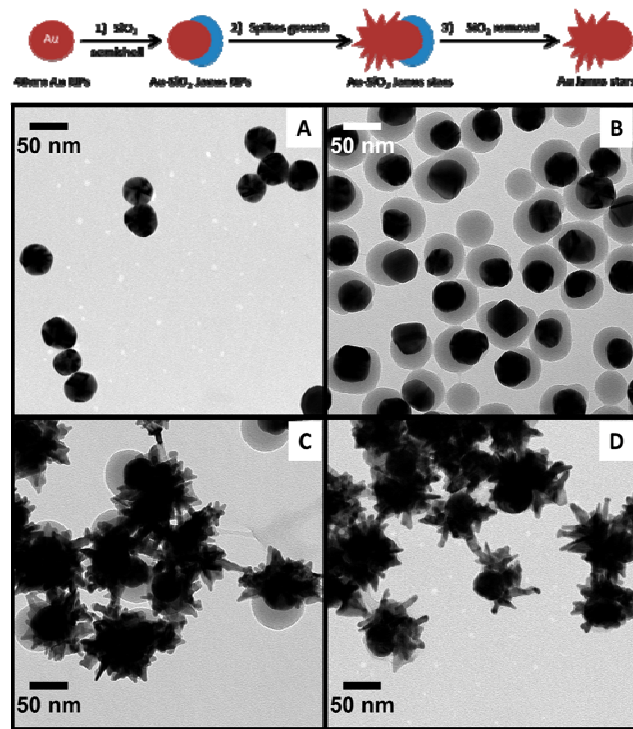


Fig. 1. Representative TEM micrographs of: ~40nm Au@citrate (A); Janus Au-SiO₂ (B); Au-SiO₂ Janus nanostars (C); and Au Janus nanostars after SiO₂ removal (D). See low magnification images in *Figure S1* (ESI).

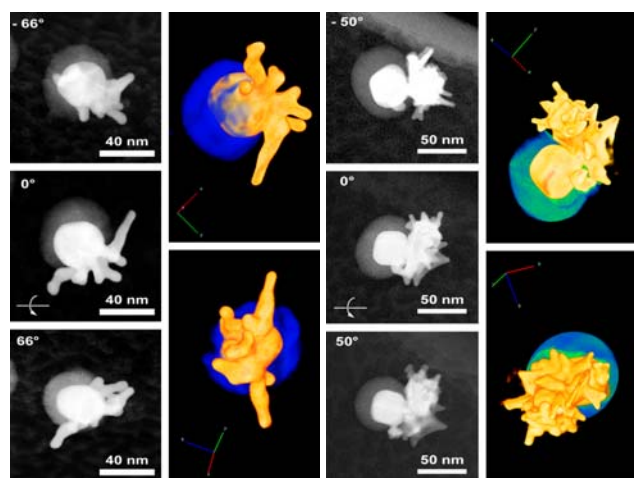


Fig. 2. HAADF-STEM images used for tomographic reconstruction acquired at different angles and the corresponding rendered 3D reconstructions along different directions, showing the Au parts in yellow and the SiO₂ shells in blue, for two different Au-SiO₂ Janus stars (left: short branches; right: large branches).

($\lambda_{\text{max}} \sim 535\text{nm}$) are shown in *Figure 1B* and *S2*, respectively. The TEM micrographs nicely show the formation of silica semishells on the Au cores, with minor silica nucleation, which did not affect the subsequent synthesis steps, while the plasmon band shows a small redshift due to changes in the local refractive index around the Au nanoparticle cores.¹² The SiO₂ semishell was subsequently used as a hard mask to protect part of the surface against the further growth of Au spikes (*step 2, Figure 1*). Upon centrifugation and washing with pure water, Au spikes were grown using a surfactant-free approach, where L-ascorbic acid acts as a weak reducing agent in the presence of AgNO₃ and HCl (aq).¹³ We observed that spikes can only be grown in the presence of silver ions, and otherwise metal overgrowth takes place without branches formation (see *Figure S6*). Since this method avoids the use of surfactants and polymers, exchange of the remaining PAA is not needed and the obtained branched structures display a rather clean surface, which makes them ideal candidates for self-assembly or surface enhanced Raman scattering (SERS), where subsequent functionalization is usually required.^{14,15,16,17,18} Au-SiO₂ Janus nanostars were obtained in less than one minute and collected by centrifugation. It has been reported that, after several hours to days such nanostars may undergo a reshaping process, leading to less spiky structures, which is reflected in a plasmon band blueshift.¹⁹ In these surfactant-free stars this process was observed within a couple of days and additionally the silica semishell was found to dissolve if the particles were stored in aqueous solution after the synthesis (see *Figures S3* and *S4*).²⁰ However, both processes can be prevented by transferring the particles into an ethanol solution containing 4-MBA (20 μM) and washing several times with pure ethanol to remove unattached 4-MBA molecules. As can be observed in *Figure 1C*, the silica shell and the spikes are still present in particles prepared in this way. The choice of 4-MBA relies on the well-known adsorption of thiol molecules over metal surfaces, which prevents other surface phenomena from occurring, as reflected in the stability of the gold spikes, which remained unchanged for at least three months. Storage of Au-SiO₂ Janus stars in water without addition of 4-MBA however

leads to less spiky structures and silica dissolution within a few 40 days (see *Figure S4*). Oppositely, upon addition of 4-MBA in water Au Janus nanostars were obtained, i.e. the Au branches were preserved while the silica protecting mask was removed (*step 3, Figure 1*). A representative TEM image of these Au Janus nanostars is shown in *Figure 1D*, where the branches can 45 be seen next to a smooth gold hemisphere.

Since conventional TEM images only provide 2D projections of 3D objects, more detailed characterization was carried out by high-angle annular dark-field scanning transmission electron microscopy (HAADF-STEM) tomography (see *rendered movies* 50 *in ES†*), and aberration corrected high resolution HAADF-STEM to clarify their morphology. Two examples are shown in *Figure 2* for Au-SiO₂ Janus nanostars with short and long branches, for which we display HAADF-STEM images obtained at different angles, together with the corresponding rendered 3D images. Silica is represented in blue and the metallic part in golden colour. These images clearly confirm that the gold spikes only grow from the exposed face of the metal, which was not covered by the silica hard mask (protecting group). Whereas for short spikes random orientation from the central core is observed, in 60 the long branched nanoparticles, obtained when using lower amount of seeds, the 3D structure suggests that secondary branching occurred on few spikes that were initially grown from the core. This cannot be observed in conventional TEM projection images, so HAADF-STEM tomography is an essential 65 tool to understand this type of systems. Tomography was also used to image the Janus nanostars after dissolution of the silica shell, again clearly showing a highly branched side, which is well differentiated from a quasi-spherical side (see *Figure S7*).

A final piece of information regarding the ultrastructure of 70 these unusual nanoparticles was provided by high resolution HAADF-STEM, as exemplified in *Figure 3*. A HAADF-STEM image of a single Au-SiO₂ Janus star with small branches is shown in *Figure 3A*, revealing the presence of a spherical gold core from which spikes protrude (bright areas) 75 and a silica semishell (faint grey area). The more detailed image of the same particle in *Figure 3B* indicates that the gold core is multiply twinned, as expected for such large quasi-spherical particles, whereas the images in *Figure 3C-D* show the branching part from the core for several spikes, indicating 80 that they are single crystalline. Paying more attention to the edge of the spike in *Figure 3D*, deviation from the zone axis orientation can be seen, so highly branched particles might exhibit different crystallographic orientations where secondary spikes grow over previous branches. A similar 85 analysis was carried out on particles with larger branches (see *Figure S8*), but in this case the overlap between different parts of the particles makes it difficult to distinguish the corresponding crystallographic orientations.

Regarding the optical response of these anisotropic 90 nanostructures, the Vis-NIR spectra of colloids obtained with different amounts of seeds (*Figure S2*) show that the main plasmon band is more redshifted for lower amounts of seeds, in good correlation with the growth of longer branches, as previously reported.^{18,21,22} It should be noted that the amount 95 of seeds is also a critical parameter to optimize branched growth without secondary nucleation. Closer attention to the

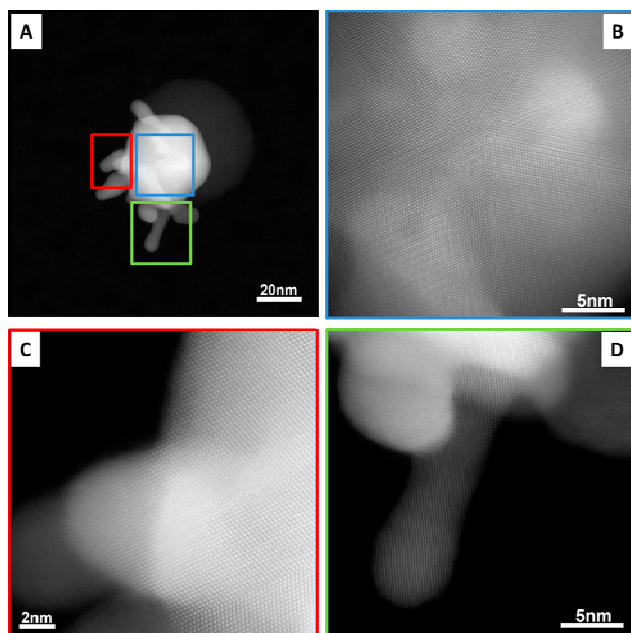


Fig. 3. **A)** HAADF-STEM image of a single Au-SiO₂ Janus nanostar with short spikes, revealing the presence of a gold core with branches (brighter features) and also a SiO₂ shell at one side of the particle (faint grey area). **B-D)** HRSTEM images of the same particle showing that the Au core is multi-twinned whereas the branches are single crystals.

Vis-NIR spectra reveals that they comprise two localized surface plasmon resonance (LSPR) bands,¹⁸ which is typical for star-like nanoparticles. The LSPR mode around 540 nm depends on core size, in this case determined by the original Janus seeds, whereas the second mode is focalized at the tips and its position can be tuned between 700-850 nm by simply changing the amount of seeds (and in turn branch dimensions). Other parameters such as the addition of HCl or the amount of Ag⁺ ions can also modify the morphology and affect the LSPR position, but we have found that tuning the seeds concentration is a more reliable and reproducible strategy. When comparing these spectra with those of standard Au nanostars, it seems that the relative intensities between tip to core LSPR modes is lower in the Janus nanostars, which can be due to the smaller amount of branches per particle compared to standard nanostars. This agrees with theoretical modelling indicating that the intensity of the tip mode is proportional to the number of spikes.¹⁸

In summary, we have demonstrated application of the protecting group concept for the synthesis of Janus nanoparticles comprising a spherical gold core half covered with a silica semishell and with gold tips branching out from the other half. Advances on the colloidal synthesis of Janus particles allowed us to deposit silica half shells on metallic spheres, which were then used as hard masks to prevent the growth of gold spikes over the whole surface. The mask can be easily removed by dissolving silica in aqueous solution, thus completing the similarity with protecting groups in Organic chemistry. These particles exhibit optical properties similar to those of gold nanostars in solution, but enhanced anisotropy can be expected for oriented assemblies by exploiting the Janus conformation. We have also shown that aberration corrected HAADF-STEM imaging and tomography

are essential tools to disclose the Janus morphology. Applications can be envisaged in e.g. surface enhanced spectroscopies or in the design of colloidal swimmers.

This work was supported by the EU (ESMI, grant number FP7-INFRASTRUCT-2010-1, 262348) and the European Research Council (PLASMAQUO, 267867). D.R.-F. acknowledges an FPU fellowship from The Spanish MECD. The authors acknowledge thank Dr. M. Grzelczak for useful suggestions.

Notes and references

- ^a BioNanoPlasmonics Laboratory, CIC biomaGUNE, Paseo de Miramón 182, 20009 Donostia – San Sebastián, Spain. Fax: 34 943005301; E-mail: lizmarzan@cicbiomagune.es.
^b EMAT-University of Antwerp, Groenenborgerlaan 171, B-2020, Antwerp, Belgium
^c Departamento de Química Física, Universidade de Vigo, 36310 Vigo, Spain
^d Ikerbasque, Basque Foundation for Science, Bilbao, Spain.

Electronic Supplementary Information (ESI) available: [Experimental procedures, additional TEM images and Vis-NIR spectra, control experiments] See DOI: 10.1039/b000000x/

- G.M. Wuts, T.W. Greene, Protective Groups in Organic Synthesis, 4th ed., John Wiley & Sons Inc., Hoboken, New Jersey, 2007.
- A. Perro, S. Reculosa, F. Pereira, M.-H. Delville, C. Mingotaud, E. Duguet, E. Bourgeat-Lamid, S. Ravaine, *Chem. Commun.*, 2005, 5542.
- X. Xu, N. L. Rosi, Y. Wang, F. Huo, C. A. Mirkin, *J. Am. Chem. Soc.*, 2006, **128**, 9286.
- M. M. Maye, D. Nykypanchuk, M. Cuisinier, D. van der Lelie, O. Gang, *Nat. Mater.*, 2009, **8**, 388.
- F. Wang, S. Cheng, Z. Bao, J. Wang, *Angew. Chem. Int. Ed.* **2013**, 52, 1.
- A. Guerrero-Martínez, M. Grzelczak, L.M. Liz-Marzán, *ACS Nano*, 2012, **6**, 3655.
- A. Guerrero-Martínez, S. Barbosa, I. Pastoriza-Santos, L.M. Liz-Marzán, *Curr. Op. Colloid Interface Sci.*, 2011, **16**, 118.
- D. Rodríguez-Fernández, L. M. Liz Marzán, *Part. Part. Syst. Charact.*, 2013, **30**, 46.
- N. G. Bastús, J. Comenge, V. Puentes, *Langmuir*, 2011, **27**, 11098.
- G. Frens, *Nat. Phys. Sci.*, 1973, **241**, 20.
- T. Chen, G. Chen, S. Xing, T. Wu, H. Chen, *Chem. Mater.*, 2010, **22**, 3826.
- L. M. Liz Marzán, M. Giersig, P. Mulvaney, *Langmuir*, 1996, **12**, 4329.
- H. Yuan, C. G. Khoury, H. Hwang, C. M. Wilson, G. A. Grant, T. Vo-Dinh, *Nanotechnology*, 2012, **23**, 075102.
- S. Chen, Z. L. Wang, J. Ballato, S. H. Foulger, D. L. Carroll, *J. Am. Chem. Soc.*, 2003, **125**, 16186.
- E. Hao, R. C. Bailey, G. C. Schatz, J. T. Hupp, S. Li, *Nano Lett.*, 2004, **4**, 327.
- T. K. Sau, C. J. Murphy, *J. Am. Chem. Soc.*, 2004, **126**, 8648.
- J. Xie, J. Y. Lee, D. I. C. Wang, *Chem. Mater.*, 2007, **19**, 2823.
- P. S. Kumar, I. Pastoriza-Santos, B. Rodríguez-González, F. J. García de Abajo, L. M. Liz-Marzán, *Nanotechnology*, 2008, **19**, 015606.
- L. Rodríguez-Lorenzo, J. M. Romo-Herrera, J. Pérez-Juste, R. A. Álvarez-Puebla, L. M. Liz-Marzán, *J. Mater. Chem.*, 2011, **21**, 11544.
- Y. J. Wong, L. Zhu, W. S. Teo, Y. W. Tan, Y. Yang, C. Wang, H. Chen, *J. Am. Chem. Soc.*, 2011, **133**, 11422.
- F. Hao, C. L. Nehl, J. H. Hafner, P. Nordlander, *Nano Lett.*, 2007, **7**, 729.
- W. Y. Ma, H. Yang, J. P. Hilton, Q. Lin, J. Y. Liu, L. X. Huang, J. Yao, *Opt. Express*, 2010, **18**, 843.